EFDA–JET–PR(09)44

V.D. Pustovitov, F. Villone
and JET EFDA contributors

Effect of Ferromagnetic Structures on RWM Growth Rates: A Cylindrical Model and a Verification on JET

Effect of Ferromagnetic Structures on RWM Growth Rates: A Cylindrical Model and a Verification on JET

V.D. Pustovitov[1], F. Villone[2] and JET EFDA contributors*

JET-EFDA, Culham Science Centre, OX14 3DB, Abingdon, UK

[1]Institute of Tokamak Physics, Russian Research Centre "Kurchatov Institute", Kurchatov Sq., 1, Moscow, 123182, Russian Federation
[2]Associazione EURATOM/ENEA/CREATE, DAEIMI, Università di Cassino, Via Di Biasio 43, 03043, Cassino (FR), Italy
** See annex of F. Romanelli et al, "Overview of JET Results", (Proc. 22 [nd] IAEA Fusion Energy Conference, Geneva, Switzerland (2008)).*

Preprint of Paper to be submitted for publication in
Plasma Physics and Controlled Fusion

ABSTRACT

The Resistive Wall Mode (RWM) dispersion relation is analytically derived for a cylindrical plasma surrounded by two walls: the first wall (facing the plasma) is assumed thin (geometrically and magnetically) and resistive, while the second wall of larger radius is ferromagnetic, but nonconductive. The predictions of this simplified model are verified on the JET tokamak, by a comparison with the calculations of a linearized axisymmetric plasma response model. In this case, it is found that, assuming all active and passive conducting structures as short circuited, the presence of iron causes a constant increase of the n=0 RWM growth rate of around 25 s^{-1}, independently of the plasma configuration under study.

1. INTRODUCTION

The Resistive Wall Mode (RWM) is an ideal external kink mode that gets unstable, e.g. when the plasma pressure exceeds a given threshold. Thanks to the presence of conducting structures surrounding the plasma, the growth rate of the mode is typically of the order of the inverse of the magnetic diffusion time in the conductors.

This mode is of particular concern for ITER [1], since for long pulse operation the RWM instability, if not properly controlled, can pose a severe limitation in terms of the achievable plasma pressure. Consequently, significant modelling efforts have been devoted to understanding the present experimental results and to extrapolating the RWM behaviour to ITER. Several codes have been developed in the last years [1]; here we mention the CarMa code [2], which can study RWM by solving linearized ideal MHD equations in presence of three-dimensional volumetric conducting structures. This code has been validated on experimental results [3], and includes plasma flow and kinetic damping [4].

Available analytical and computational models for RWM studies usually do not allow the treatment of ferromagnetic properties. One of the reasons is that they are based on the thin-wall approximation (constant normal component $\mathbf{b}\cdot\mathbf{n}_w$ of the perturbation $\mathbf{b}$ across the wall) which prevents proper incorporation of the permeability effects [5]. Studying the ferromagnetic effects on plasma stability requires, therefore, a full volumetric treatment of the conducting structures, such that can be done by the aforementioned code CarMa. Although the enhancement of the electromagnetic formulation to ferromagnetic materials is already available [6], the overall CarMa code, taking also plasma response into account, has not been upgraded yet in this respect.

The subject attracted attention because ferromagnetic materials can be in fact present in existing devices, like the JET tokamak [8]. Furthermore, in ITER the presence of ferromagnetic steel is envisaged [1] in test blanket modules in view of its high tolerance against neutron irradiation and high heat conduction. Also, ferromagnetic inserts can be used (with an

appropriate arrangement) for the toroidal field ripple reduction [1, 8]. On the other hand, there is a concern about possible destabilizing effect of these ferritic elements on ITER plasmas [1] which requires systematic study of the problem.

The precise evaluation of these effects in realistic geometries is obviously very important for the design of feedback control systems of present-day and future devices. To this purpose, complex numerical tools are needed, e.g. the aforementioned CarMa code enhanced to take into account ferromagnetic materials, which is not available yet. Anyway, analytical results in simplified geometries can be extremely useful, not only for the trivial purpose of code benchmarking, but especially for providing a deeper insight in the general features of the phenomenon under study – in this case, the effect of ferromagnetic materials on the RWM growth rate.

In particular, recently a cylindrical model has been developed [5], taking into account ferromagnetic conducting shell circumventing the plasma; this model has confirmed their destabilizing effect on RWM growth rate and gave parametrical dependencies and quantitative estiamtes. In this paper, first of all we extend this model to the case in which there are two separated walls, and the second ferromagnetic wall is non-conducting. Indeed, this is usually the case, because the ferromagnetic materials near the first wall in tokamaks are laminated [8], precisely in order to minimize eddy currents losses. Also, in ITER such materials will be segmented in the toroidal and poloidal directions [1]. Thanks to this simplification, the RWM dispersion relation derived here assumes a particularly concise form, predicting that the RWM growth rate is augmented by a quantity which does not depend on the plasma configuration under consideration.

This analytical prediction is confirmed by several calculations made on the JET geometry with CREATE_L [9], a linearized axisymmetric perturbed equilibrium code. This way, we also quantify the destabilizing effect of iron on the growth rates of axisymmetric vertical instabilities at JET, taking into account a very realistic (although axisymmetric) geometrical description of the various metallic structures surrounding the plasma.

The paper is organized as follows. In Section 2 we introduce the cylindrical model and derive the dispersion relation, which is discussed in Section 3. In Section 4 we present the results on the JET geometry and, finally, Section 5 draws the conclusions.

2. DISPERSION RELATION IN THE CYLINDRICAL MODEL

For analytical evaluation we consider the plasma surrounded by two walls as a cylindrical configuration. The first wall (facing the plasma) is assumed thin (geometrically and

magnetically) and resistive, while the second wall of larger radius is ferromagnetic, but nonconductive.

Similar configuration with two walls was treated in [10, 11, 12], but in those cases both conducting walls were considered nonferromagnetic. In [5] a single resistive ferromagnetic wall was considered to analyze the RWM experiments in the Wisconsin rotating wall [13]. Neither of these models can give us the result for the case we study here. However, we can substantially base our derivations here on the results and procedures from the previous works, so that only most important and new elements of the model will be presented below.

In the model, the radial component of the magnetic perturbation **b** is expressed as a set of harmonics,

$$b_r = \sum b_{mn}(r,t)\exp(im\theta - in\zeta), \tag{1}$$

with $\zeta = z/R$ staying for the 'toroidal angle' ($2\pi R$ is the length of equivalent torus), r, θ, and z being the cylindrical coordinates related to the axis of symmetry.

If the first wall can be considered as a thin resistive shell of radius $r = r_{w1}$, the dynamics of the magnetic perturbation can be described by the equation [10, 14, 15, 16]

$$\tau_w \frac{\partial B_m}{\partial t} = \Gamma_m^{w1} B_m - \Gamma_m^0 B_m^{ext1}, \tag{2}$$

where (assuming no currents between the plasma and the first wall)

$$B_m \equiv b_{mn}(r_{w1},t) = B_m^{pl} + B_m^{w1} + B_m^{ext1} \tag{3}$$

is the amplitude of the (m,n) harmonic of the radial perturbed magnetic field at the first wall, B_m^{pl} is the contribution to $B_m(t)$ from the plasma, B_m^{w1} is the field produced by the currents in the first wall, and B_m^{ext1} is the part of B_m created by all possible sources behind the first wall (in the region $r > r_{w1}$). The other symbols:

$$\tau_w = \mu_0 \sigma r_{w1} d \tag{4}$$

is the 'wall time' in the thin-wall approximation, $\mu_0 = 4\pi \cdot 10^{-7}$ H/m is the permeability of vacuum, σ is the wall conductivity, d is the thickness of the first wall,

$$\Gamma_m^{w1} \equiv \Gamma_m^0 (1 - B_m^{pl}/B_m) \tag{5}$$

is a complex quantity describing the plasma response to the applied perturbation ($\Gamma_m^{w1} = 0$ if $B_m = B_m^{pl}$, which means no external sources),

$$\Gamma_m^0 \approx -2|m| \tag{6}$$

for $m \neq 0$ and $\Gamma_m^0 \approx -2$ when $m = 0$. In the following we assume $m > 0$.

The parameter Γ_m^{w1} introduced by (5) can be can be experimentally measured [17, 18] by means of magnetic spectroscopy diagnostics. It can also be related to the solution for b_{mn} inside the plasma as described in [15, 18, 19, 20]. Indeed, in the plasma-wall vacuum gap we have

$$\frac{rb'_{mn}}{b_{mn}} = -(m+1) - \frac{2m\Gamma_m^{w1} x^{2m}}{2m + \Gamma_m^{w1}(1-x^{2m})}, \tag{7}$$

where the prime means the radial derivative ($m > 0$ here and below). It follows from (7) that Γ_m^{w1} can be expressed through rb'_{mn}/b_{mn} at the outer side of the plasma surface S_{pl}, $x = r_p / r_{w1}$ where r_p is the plasma minor radius. This formula was obtained using the vacuum solution for b_{mn}. If there are no surface currents at the plasma boundary, rb'_{mn}/b_{mn} must be continuous there, so that both solutions for b_{mn}, in vacuum ($r > r_p$) and inside the plasma ($r < r_p$), give the same rb'_{mn}/b_{mn} at $r = r_p$. Very often, however, the plasma is described by the ideal or resistive MHD equations with sharp boundary plasma-vacuum. This implies a jump in rb'_{mn}/b_{mn} at S_{pl}, which calculation is an important part of MHD approaches. Such a jump occurs, for example, when there is a finite current density at the plasma edge. For uniform current density in the plasma we obtain with account of this jump:

$$\Gamma_m^{w1} = -2m\frac{m - nq - 1}{m - nq - 1 + \alpha}, \tag{8}$$

where $\alpha \equiv (r_p / r_{w1})^{2m}$. This corresponds to Eq. (27.13) in [21], Eq. (6) in [22], Eq. (33) 12] and Eq. (38) in [23]. This formula proved to be useful in analytical studies and for testing the codes.

The field from external sources can be represented in the form

$$B_m^{ext1} = B_m^{er} + B_m^{CC} + B_m^{w2} \tag{9}$$

with B_m^{CC} describing the pre-programmed field produced by the active (correction) coils, B_m^{er} the amplitude of the (m,n) error field harmonic, and B_m^{w2} the contribution from the second wall (in a general case, from all other sources at $r > r_{w1}$). It is B_m^{w2} in (9) that makes our analysis different from the cases considered earlier.

Our purpose here is evaluation of the second (nonconducting ferromagnetic) wall effect on the plasma stability, so we assume $B_m^{er} + B_m^{CC} = const$, in which case this quantity will not affect the dispersion relation provided that $\Gamma_m^{w1} = const$. The latter condition means a linear plasma response, which can be seen from (5), and constant $B_m^{er} + B_m^{CC}$ will only affect the stationary

level of B_m. With these assumptions, the varying part of B_m^{ext1}, which we need in (2) to get a dispersion relation, is B_m^{w2}.

To make (2) an equation for B_m, we have to find B_m^{w2} as a function of B_m. The second wall of radius $r = r_{w2} > r_{w1}$ is assumed nonconducting, but ferromagnetic. For its description we can use, with proper reduction, the results of the paper [5]. In particular, equation (33) from [5], which we rewrite here in the form (disregarding the time derivative since, by assumption here, the conductivity of this wall is zero)

$$(\Gamma_m^{w2} - \Gamma_m^c)\psi_- + 2m\psi_m^{ext2} = 0, \tag{10}$$

where ψ_m is a function related to the magnetic perturbation by $b_{mn} = im\psi_m / r$, $\psi_- = \psi_m(r_{w2})$,

$$\Gamma_m^c = \Gamma_m^\infty \frac{\psi_- - \psi_+ y_+^{-m}}{\psi_-} \tag{11}$$

with

$$\Gamma_m^\infty \equiv -m\frac{\hat{\mu}-1}{\hat{\mu}} \tag{12}$$

and $\hat{\mu} \equiv \mu / \mu_0$ (μ is the magnetic permeability of the second wall), while $\psi_+ = \psi_m(r_{w2} + d_{w2})$ and $y_+ = 1 + d_{w2}/r_{w2}$ with d_{w2} being the thickness of the second wall. The other quantities in equation (10) are Γ_m^{w2}, defined by equation (27) from [5], which can be reduced to

$$\Gamma_m^{w2} \equiv -2m\frac{\psi_m^{ext1}}{\psi_m}\bigg|_{w2-} = -2m\frac{b_m^{ext1}}{b_m}\bigg|_{w2-}, \tag{13}$$

where '$w2-$' denotes the inner side of the second wall, $\psi_m^{ext1} \equiv \psi_m^{w2} + \psi_m^{ext2}$ with ψ_m^{w2} being the contribution to ψ_m from the second wall, and ψ_m^{ext2} the part of ψ_m produced by the external sources behind the second wall.

Here we assume $\psi_m^{ext2} = 0$, then we have from (10)

$$\Gamma_m^{w2} = \Gamma_m^c, \tag{14}$$

while Γ_m^c for this case and with $\sigma_{w2} = 0$ (which means no induced currents in the second wall) is given by equation (53) from [5]:

$$\Gamma_m^c \equiv -m\frac{\hat{\mu}^2 - 1}{\hat{\mu}}\frac{1-\varepsilon_w}{\hat{\mu}+1-\varepsilon_w(\hat{\mu}-1)}, \tag{15}$$

where

$$\varepsilon_w \equiv y_+^{-2m} = \left(\frac{r_{w2}}{r_{w2}+d_{w2}}\right)^{2m}. \tag{16}$$

The latter equations show that, in the case considered, Γ_m^{w2} is a constant depending on m, ε_w and $\hat{\mu}$ only.

Now we can use equation (13) to find B_m^{ext1}. This can be done with account of

$$b_m = B_m^{in} x^{-m-1} + B_m^{ext1} x^{m-1}, \tag{17}$$

which describes b_m between the two walls. Here $x \equiv r / r_{w1}$, B_m^{in} and B_m^{ext1} are the time-dependent constants (amplitudes at $r = r_{w1}$) describing, respectively, the contribution to b_m from the inner region, which means here $r < r_{w2}$ (plasma and the first wall), and from the outer, $r \geq r_{w2}$ (the second wall). By definition, the amplitude of the total perturbation is $B_m = B_m^{in} + B_m^{ext1}$. Therefore, (17) can be rewritten as

$$b_m = B_m x^{-m-1} + B_m^{ext1}(x^{m-1} - x^{-m-1}). \tag{18}$$

With this relation and $b_m^{ext1} = B_m^{ext1} x^{m-1}$ (here it is the contribution to b_m from the second wall) we transform (13) to

$$\Gamma_m^{w2} = -2m \frac{B_m^{ext1} x_2^{2m}}{B_m + B_m^{ext1}(x_2^{2m} - 1)}, \tag{19}$$

where $x_2 \equiv r_{w2} / r_{w1}$. Since $\Gamma_m^0 = -2m$, this gives

$$\Gamma_m^0 B_m^{ext1} = -\Delta\Gamma_m^f B_m, \tag{20}$$

where

$$\Delta\Gamma_m^f \equiv \frac{\Gamma_m^c \Gamma_m^0}{\Gamma_m^c (x_2^{2m} - 1) - \Gamma_m^0 x_2^{2m}}, \tag{21}$$

Γ_m^c stays for Γ_m^{w2} since, for the case considered, $\Gamma_m^{w2} = \Gamma_m^c$, as given by (14), and Γ_m^c is defined by (15).

With $\Gamma_m^0 B_m^{ext1}$ from (20) the starting equation (2) turns into

$$\tau_w \frac{\partial B_m}{\partial t} = (\Gamma_m^{w1} + \Delta\Gamma_m^f) B_m. \tag{22}$$

For $\psi_m \propto \exp(\gamma t)$ this gives us a dispersion relation

$$\gamma \tau_w = \Gamma_m^{w1} + \Delta\Gamma_m^f, \tag{23}$$

where the second term on the right hand side describes a shift of the stability boundary due to the second (nonconducting ferromagnetic) wall.

3. DISCUSSION

3.1. Asymptotic values

First of all, we consider several asymptotic limits and the respective dispersion relations.

When $\hat{\mu}=1$, we have $\Delta\Gamma_m^f=0$, which provides the reference case with no ferromagnetic wall. With $\hat{\mu}=1$ and no currents in it the second wall is equivalent to vacuum.

We also obtain from (21) $\Delta\Gamma_m^f\to 0$ at $x_2\to\infty$ for arbitrary $\hat{\mu}$ and finite Γ_m^c, which means that the second wall at infinity gives no effect.

When $\hat{\mu}\to\infty$, from (15) we have $\Gamma_m^c=-m$. Then (21) reduces to

$$\Delta\Gamma_m^f=\frac{2m}{x_2^{2m}+1}, \tag{24}$$

and the dispersion relation (23) turns into

$$\gamma\tau_w=\Gamma_m^{w1}+\frac{2m}{x_2^{2m}+1}. \tag{25}$$

Here the second wall effect depends only on the position of this wall relative to the first wall. The last term here gives m when $x_2=1$ (the second wall is placed just behind the first wall) and zero when $x_2\to\infty$.

If the second wall (with arbitrary $\hat{\mu}$) is placed just behind the first wall, which means $x_2=1$, equation (21) is reduced to

$$\Delta\Gamma_m^f=-\Gamma_m^c. \tag{26}$$

Then (23) yields

$$\gamma\tau_w=\Gamma_m^{w1}-\Gamma_m^c. \tag{27}$$

Expression (15) gives Γ_m^c as a function of $\hat{\mu}$ and the wall thickness, d_{w2}/r_{w2}. Note that $\Gamma_m^c=0$ for $\hat{\mu}=1$, while for $\hat{\mu}\to\infty$ we have $\Gamma_m^c=-m$.

The thickness of the second wall enters the problem through ε_w defined by (16). According to (15), Γ_m^c is small when the wall is very thin ($\varepsilon_w\approx 1-2md_{w2}/r_{w2}$) and increases to

$$\Gamma_m^c=-m\frac{\hat{\mu}-1}{\hat{\mu}} \tag{28}$$

when $\varepsilon_w\to 0$ (very thick wall).

3.2. Growth rate

The dispersion relation (23) let us conclude that the presence of a ferromagnetic non-conducting shell always enhances the RWM growth rate (hence is always destabilizing):

$$\gamma = \gamma_0 + \Delta\gamma \tag{29}$$

$$\gamma_0 \tau_w = \Gamma_m^{w1}, \quad \Delta\gamma\tau_w = \Delta\Gamma_m^f \tag{30}$$

where γ_0 (resp. γ) is the growth rate without (resp. with) the ferromagnetic shell, and $\Delta\gamma$ is the related growth rate increase. Destabilizing influence of the resistive ferromagnetic wall on the plasma was also found in analytical studies [13, 24, 25] reviewed in [5], all for simpler geometries than the considered here.

In our case the growth rate increase normalized with the wall time $\Delta\gamma\tau_w$ depends on the following four physical parameters:

- the poloidal mode number *m*;
- the relative ferromagnetic wall thickness d_{w2}/r_{w2};
- the second wall position r_{w2}/r_{w1} relative to the first wall;
- the magnetic permeability $\hat{\mu}$ of the ferromagnetic wall.

We stress explicitly that the quantity $\Delta\gamma\tau_w$ does not depend on the plasma response details, nor on the toroidal mode number – these quantities influence only γ_0. We stress that these qualitatively very concise results depend crucially on the assumption that no current density can be induced in the ferromagnetic shell, since it is not conducting, so that no time dynamics is involved there. Otherwise we would obtain second-order equation [10, 11, 12], while (23) is linear.

4. VERIFICATION ON JET GEOMETRY

Due to the generality of the above considerations, we verify these findings on the JET tokamak. We concentrate on *n*=0, *m*=1 RWM (axisymmetric vertical instability), that we describe with the CREATE_L axisymmetric linearized plasma response model [CL]. This model solves linearized Grad-Shafranov equations around a given reference equilibrium configuration, providing a state-space model from which the growth rate of the vertical instability can be easily derived.

The JET tokamak [JET] has a non-linear ferromagnetic structure circumventing the plasma. Its main purpose is to facilitate the transformer action of current inducing PF coils. Fig. 1 shows the reference geometry in the poloidal plane, reporting the iron cross-section as well as the various active and passive conductors and one of the plasma configurations considered. A rather accurate description of the geometry is implemented, and the resulting CREATE_L model has been successfully validated against experimental results [26]. This model is also extensively used during JET experimental campaigns for the derivation of the so-called eXtreme Shape Controller (XSC) [27] and for vertical position stabilization [28].

We notice that the *n*=0 RWM growth rates predicted by the CREATE_L model are in excellent agreement with the experimental findings, over a very wide range of values, as

reported in [26] and [29]. In particular, in [29] the experimental growth rates have been measured in dedicated experiments, in which the plasma evolved with no vertical control active, giving rise to an exponential vertical movement till the termination of the shot.

We consider five equilibrium configurations, corresponding to plasmas with rather different parameters, which is reflected in very different growth rates of the vertical instability – see Table 1 for details. For each of these configurations, we compute the reference equilibrium including the non-linear B-H curve of the ferromagnetic material, reported in [26]. Then, we calculate the linearized plasma response around these equilibria, first including the ferromagnetic material (of course linearizing the iron characteristic), and then assuming fictitiously that no magnetic material is present. The first calculation provides the quantity γ and the second one γ_0, the difference giving precisely $\Delta\gamma$. In doing these computations both the active coils and the passive conductors (vessel, mechanical structure etc.) shown in Fig. 1 have been assumed as short-circuited.

The results are reported in Table 1. Evidently, despite the fact that the geometry is very far from a cylinder, nevertheless the qualitative result that $\Delta\gamma$ does not depend on the plasma configuration is clearly confirmed. Indeed, even with a variation of growth rate of a factor more than two (i.e. with very different plasma configurations) the quantity $\Delta\gamma$ varies only around 15%. These small variations of $\Delta\gamma$ can be mainly attributed to the fact that the relative position of the plasma centroid varies in these cases, hence modifying the equivalent radius of the vessel (conducting wall) and of the iron (ferromagnetic shell).

To sum up, we can quantify the (constant) growth rate increase due to the presence of iron in JET, as around 25 s^{-1}, assuming all active and passive conducting structures as short circuited. This increase is evidently relatively less important for the most unstable plasmas, i.e. the most dangerous configurations from the stabilization point of view. However, we stress that it would be not correct to conclude that the presence of iron can be neglected in stabilization studies at JET and in other devices. Indeed, it is fundamental to properly take into account the presence of ferromagnetic materials for at least two aspects: equilibrium calculation and feedback studies. In particular, in the first case it is crucial even to correctly treat the non-linear magnetic characteristic, e.g. properly considering the saturations. In the last case, we may argue that in general both the dynamical response of an active coil used for feedback control and its magnetic field pattern are in general significantly affected by the presence of ferromagnetic materials.

5. CONCLUSIONS

In this paper we have derived the dispersion relation of RWM, for a cylindrical plasma circumvented by a thin resistive shell and an outer, non-conducting, ferromagnetic wall. We

demonstrated that the resulting growth rate is always greater than that in absence of ferromagnetic materials, hence always providing a destabilizing effect, which is consistent with previous results similarly obtained for somewhat different arrangements [5]. In the case considered here the growth rate increase does not depend on the plasma configuration, but only on the poloidal mode number and on physical and geometrical properties of the ferromagnetic shell.

We have verified these findings with several calculations of the axisymmetric vertical instability growth rates on the JET tokamak with the CREATE_L code. Although the JET geometry is very different from the simplified case treated analytically, nevertheless the main qualitative conclusion is absolutely confirmed. This shows once again, in addition to the ITER-relevant cases [1], the importance of analytical results on RWM, which are able to highlight some features that cannot be easily extracted even with detailed numerical tools.

We have quantified the constant growth rate increase due to iron in JET as around 25 s^{-1}, assuming all active and passive conducting structures as short circuited. Note that $\Delta\gamma/\gamma << 1$ for the JET shots shown in Table 1 well agrees with a general conclusion [5] that the ferromagnetic destabilizing effect in tokamaks must be a small negative shift of the stability boundary, just several percent. With known $\Delta\gamma$ it can be, in principle, easily counteracted by the feedback system, especially when $\Delta\gamma$ remains constant in a wide range of plasma parameters.

Our analytical and numerical results also explain and confirm the results of the dedicated experiments in the JFT-2M tokamak where no adverse effect of ferritic steel on the plasma operation and stability was observed [30, 31, 32]. We prove that the encouraging conclusions [30, 31, 32] on the compatibility of reduced activation ferritic steel wall with high performance plasma, based on the JFT-2M experiments, must be valid in a case with ITER-like structures of resistive and ferritic materials.

Further work will be addressed in enhancing advanced RWM codes (like CarMa), in order to allow the treatment of ferromagnetic materials in tokamaks operating with high-beta plasmas near or above the MHD stability limits.

ACKNOWLEDGEMENTS

The authors are grateful to R Albanese and G Rubinacci for useful discussions, to V.S. Mukhovatov and Yu.V. Gribov for their continuous encouragement, and to N.V Ivanov and S.V Konovalov for the support to the work. This work was supported in parts by Consorzio CREATE, the Rosatom State Corporation and the Dutch-Russian Centre of Excellence on Fusion Physics and Technology (grant NWO-RFBR 047.018.002). This work, supported by the European Communities under the contract of Association between EURATOM and ENEA, was

carried out within the framework of the European Fusion Development Agreement. The views and opinions expressed herein do not necessarily reflect those of the European Commission.

REFERENCES

[1]. Hender T.C. *et al* 2007 *Nucl. Fusion* **47** S128

[2]. Portone A, Villone F, Liu Y Q, Albanese R and Rubinacci G 2008 *Plasma Phys. Control. Fusion* **50** 085004

[3]. Villone F, Liu Y.Q, Paccagnella R, Bolzonella T and Rubinacci G 2008 *Phys. Rev. Lett.* **100** 255005

[4]. Liu Y.Q and Villone F. *Plasma Phys. Control. Fusion* **51** 115008 (2009)

[5]. Pustovitov V.D. 2009 *Phys. Plasmas* **16** 052503

[6]. Albanese R and Rubinacci G 1998 *Adv. Im. El. Phys.* **102** 1–86

[7]. Wesson J *The science of JET* (http://www.jet.efda.org/documents/books/wesson.pdf)

[8]. Tobita K, Nakayama T, Konovalov S.V and M Sato 2003 P*lasma Phys. Control. Fusion* **45** 133

[9]. Albanese R and Villone F 1998 *Nucl. Fusion* **38** 723

[10]. Pustovitov V.D 2001 *Plasma Phys. Rep.* **27** 195

[11]. Gribov Y and Pustovitov V.D 2002 Analytical study of RWM feedback stabilisation with application to ITER *Proc. 19th IAEA Fusion Energy Conf. (Lyon, 2002)* (Vienna: IAEA) IAEA-CN-94/CT/P-12 and http://www.iaea.org/programmes/ripc/physics/fec2002/html/fec2002.htm

[12]. Bondeson A, Liu Y.Q, Gregoratto D, Gribov Y and Pustovitov V.D. 2002 *Nucl. Fusion* **42** 768

[13]. Bergerson W.F, Hannum D.A, Hegna C.C, Kendrick R.D, Sarff J.S and Forest C.B 2008 *Phys. Rev. Lett.* **101** 235005

[14]. Pustovitov V.D, 2003 *JETP Lett*. **78** 281

[15]. Pustovitov V.D, 2004 *Plasma Phys. Reports* **30** 187

[16]. Pustovitov V.D, 2004 Error field amplification in tokamaks *Theory of Fusion Plasmas, Proc. Joint Varenna-Lausanne Int. Workshop (Varenna)* (Bologna: Editrice Compositori) p 227

[17]. Reimerdes H, *et al* 2005 *Nucl. Fusion* **45** 368

[18]. Pustovitov V.D,, 2007 *Nucl. Fusion* **47** 563

[19]. Pustovitov V.D, and Mayorova M S 2006 *Plasma Phys. Control. Fusion* **48** 51

[20]. Pustovitov V.D, 2007 *Phys. Plasmas* **14** 022501

[21]. Mikhailovskii A.B, 1998 *Instabilities in a Confined Plasma* (Bristol: Institute of Physics Publishing)

[22]. Mikhailovskii A.B. and Pustovitov V.D., 2000 *Plasma Phys. Rep.* **26** 477

[23]. Liu Y.Q, Albanese R, Portone A, Rubinacci G. and Villone F, 2008 *Phys. Plasmas* **15** 072516

[24]. Bakhtiari M., *et al* 2003 *Phys. Plasmas* **10** 3212

[25]. Kurita G., *et al* 2003 *Nucl. Fusion* **43** 949

[26]. Albanese R, Mattei M and Villone F 2004 *Nucl. Fusion* **44** 999

[27]. De Tommasi G, Albanese R, Ambrosino G, Ariola M, Mattei M, Pironti A, Sartori F and Villone F 2007 *IEEE Transactions on Plasma Science* **35** 709

[28]. Sartori F *et al* 2008 *Fus. Eng. Des.* **83** 202

[29]. Villone F, Riccardo V and Sartori F 2005 *Nucl. Fusion* **45** 1328

[30]. Tsuzuki K, *et al* 2003 *Nucl. Fusion* **43** 1288

[31]. Tsuzuki K, *et al* 2006 *Nucl. Fusion* **46** 966

[31]. Tsuzuki K, *et al* 2006 *Fusion Science and Technology* **49** 197

Shot#	Centroid position [m]		Shape		Plasma parameters			Growth rates [s^{-1}]		
	R_0	Z_0	κ	δ	I_p [MA]	β_p	l_i	γ	γ_0	$\Delta\gamma$
66263	2.900	0.260	1.744	0.462	1.435	0.032	1.030	490	463	27
72147	2.915	0.229	1.677	0.382	1.432	0.051	1.150	317	293	24
75967	3.001	0.355	1.689	0.392	1.960	0.742	0.945	171	146	25
78379	2.911	0.334	1.612	0.182	1.484	0.100	1.166	324	299	25
78415	2.952	0.223	1.654	0.349	1.439	0.091	1.178	210	187	23

Table 1. JET configurations analysed: shot number, centroid position (R_0, Z_0), elongation (κ), triangularity (δ), plasma toroidal current (I_p), poloidal beta (β_p), internal inductance (l_i), and resulting growth rates.

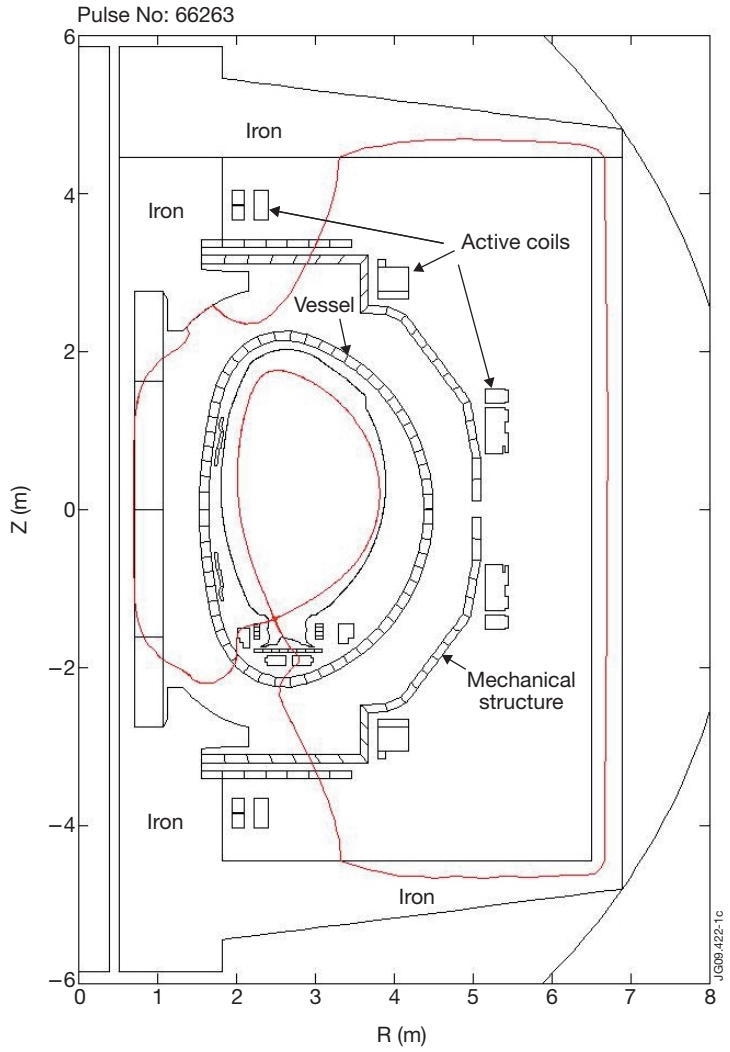

Figure 1: JET geometry and sample equilibrium. The red line shows the poloidal trace of the magnetic surface corresponding to the plasma boundary.